Biochemical and Biophysical Research Communications 447 (2014) 244–249

Contents lists available at ScienceDirect

Biochemical and Biophysical Research Communications

journal homepage: www.elsevier.com/locate/ybbrc

Cataract-linked mutation R188H promotes βB2-crystallin aggregation and fibrillization during acid denaturation

Yi-Bo Xi [a,b], Kai Zhang [c], An-Bang Dai [b], Shang-Rong Ji [a], Ke Yao [c], Yong-Bin Yan [b,*]

[a] MOE Key Laboratory of Cell Activities and Stress Adaptations, School of Life Sciences, Lanzhou University, Lanzhou 730000, China
[b] State Key Laboratory of Biomembrane and Membrane Biotechnology, School of Life Sciences, Tsinghua University, Beijing 100084, China
[c] Eye Center of the 2nd Affiliated Hospital, Medical College of Zhejiang University, Hangzhou 310009, China

ARTICLE INFO

Article history:
Received 19 March 2014
Available online 1 April 2014

Keywords:
βB2-crystallin
Inherited mutation
Autosomal dominant congenital nuclear cataract
Protein aggregation
Protein fibrillization
Acid denaturation

ABSTRACT

Cataract is characterized by the formation of light-scattering protein aggregates in the lens. β/γ-Crystallins are the predominant structural proteins in the cytosol of lens fiber cells, and more than fifty β/γ-crystallin mutations have been linked to autosomal dominant congenital cataract. However, the structural role of these mutations in the formation of the core structures of amorphous aggregates or amyloid-like fibrils has not been elucidated yet. In this research, we studied the effects of the V187M and R188H mutations on the aggregation and fibrillization of βB2-crystallin during acid denaturation. The behavior of V187M was the same as the WT protein, suggesting that the residue at position 187 contributed little to the aggregation/fibrillization process. R188H promoted the formation of amorphous aggregates at pH above 3 and accelerated fibrillization at pH 3. The distinct behaviors of the mutants suggested that the residue at position 188 might play a regulatory role in βB2-crystallin aggregation/fibrillization but not reside in the core of the aggregates/fibrils.

1. Introduction

Protein misfolding and aggregation are prevalent phenomena observed in numerous diseases, which are generally called protein folding diseases or conformational diseases [1]. The occurrence of aggregation under certain conditions can be regarded as an intrinsic property of proteins due to the marginable stability of proteins [2]. In the cells, incompletely folded proteins, misfolded proteins and aggregates are abolished by the protein quality-control system [3]. Once the aggregated proteins escape the cellular quality-control mechanism, cellular functions may be impaired by the lack of functional proteins, the toxic effects of the aggregates or the accumulation of large aggregates. Cataract, which is characterized by the opacification of the lens, is the most obvious and well-known disease caused by the appearance of large protein aggregates [4].

Lens is a highly differentiated organ with the function of transmitting and focusing light on the retina, and has been used as an excellent model to investigate fundamental biological processes for several decades [5]. In mature vertebrate lens fiber cells, the organelles are fully degraded to reduce the scattering of visible light [6]. Due to the lack of turnover machineries, the proteins in the lens are required to maintain a lifelong stability against various intracellular and environmental stresses. Consistently, crystallins, the most abundant soluble proteins in vertebrate lens, are unique in their high stability and extreme solubility up to ~300 mg/ml [7,8]. There are three classes of crystallins in vertebrate lens: α-, β- and γ-crystallins. α-Crystallins are small heat shock proteins with chaperone-like function to inhibit protein aggregation [9]. β/γ-Crystallins are structural proteins with similar tertiary structures composing four Greek-key motifs divided into two domains [7]. The major difference between β- and γ-crystallins is their oligomeric states: β-crystallins exist as homo- or hetero-oligomers, while γ-crystallins are exclusively monomers. The importance of crystallins in lens structure and function has been revealed by the extremely high concentration of crystallins in lens fiber cells and a number of cataract-linked mutations [7,10,11].

Although cataract can be induced by numerous factors, the precipitation of β/γ-crystallins is a general feature for both congenital and aging cataract. Thus, understanding crystallin aggregation is one of the key points to elucidate the molecular mechanism of cataract and to develop non-surgical methods to prevent or delay cataract [12]. In cataract lens, crystallins may deposit in amorphous

Abbreviations: ANS, 1-anilinonaphtalene-8-sulfonate; BSA, bovine serum albumin; CD, circular dichroism; DTT, dithiothreitol; EM, electron microscope; E_{max}, maximum emission wavelength of intrinsic Trp fluorescence; IPTG, isopropyl-1-thio-β-D-galactopyranoside; SEC, size-exclusion chromatography; SDS, sodium dodecyl sulfate; SDS–PAGE, SDS–polyacrylamide gel electrophoresis; ThT, thioflavin T; WT, wild type.

* Corresponding author. Fax: +86 10 6277 2245.
E-mail address: ybyan@tsinghua.edu.cn (Y.-B. Yan).

http://dx.doi.org/10.1016/j.bbrc.2014.03.119
0006-291X/

aggregates or amyloid-like fibrils. Despite of the morphological difference, the formation of both forms of aggregates is generally initiated by partially or fully unfolding of crystallins, which reorganize to pack via intermolecular β-sheet structures and grow into large aggregates thereafter [12,13]. The extensive studies in the monomeric protein γD-crystallin have led to several aggregation models depending on the conditions at which the aggregates are formed. It seems that the C-terminal domain of γD-crystallin is responsible to the formation of the core of amyloid-like fibrils, while both N- and C-terminal domain contribute to thermal aggregation [14–19]. However up to now, little is known about the details regarding the aggregation mechanism of oligomeric β-crystallins. Moreover, it is also unclear whether the cataract-linked mutations just destabilize crystallins or could play a role in the progression of aggregation. In this research, we addressed this problem by using two cataract-linked mutations (V187M and R188H) located at the last β-strand of Greek-key motif 4 in βB2-crystallin [20–22]. Acid-induced denaturation and aggregation was selected as a model system to distinguish the effects of mutations on protein stability and aggregation. Our results suggested that R188H but not V187M significantly promoted βB2-crystallin aggregation and fibrillization during acid-induced denaturation. Based on the results herein and the previous results [17,22], we proposed that His188 in the R188H mutant may promote aggregation by stabilizing intermolecular interactions among regions flanking the core of the aggregates.

2. Materials and methods

2.1. Materials

Bovine serum albumin (BSA), dithiothreitol (DTT), EDTA, isopropyl-1-thio-β-D-galactopyranoside (IPTG), sodium dodecyl sulfate (SDS), 1-anilinonaphtalene-8-sulfonate (ANS) and thioflavin T (ThT) were Sigma products. All the other chemicals were local products of analytical grade.

2.2. Protein expression and purification

The expression and purification of the wild type (WT) and mutated human βB2-crystallins were the same as those described previously [22,23]. In brief, recombinant proteins were overexpressed in *Escherichia coli* Rosetta (DE3) cells. After induction by 0.1 mM IPTG, the cells were grown in the Luria–Bertani medium for 4 h at 37 °C for the WT protein and V187M or 15 h at 20 °C for R188H. The recombinant proteins were purified from the soluble fractions of cell lysis by a Ni–NTA affinity column, followed by a Hiload 16/60 Superdex 200 prep-grade column. The purity of the final products was checked by SDS–PAGE and size-exclusion chromatography (SEC) using a Superdex 200HR 10/30 column equipped on an ÄKTA purifier. The protein concentration was determined by the Bradford method using BSA as a standard [24]. The purified proteins were dissolved in buffer A containing 20 mM sodium phosphate, 150 mM NaCl, 0.5 mM EDTA, 0.5 mM DTT. The pH of the protein solutions was adjusted by adding HCl or NaOH.

2.3. Spectroscopy

Details regarding the spectroscopic measurements were the same as those described previously [22,25]. In brief, the protein concentration was 0.2 mg/ml for all spectroscopic experiments. The high-concentration protein solutions used for fibrillization were diluted in buffer A before spectroscopic measurements. The far-UV circular dichroism (CD) spectra were measured on a Jasco J-715 spectropolarimeter. The fluorescence spectra were recorded on a Hitachi F-2500 fluorescence spectrophotometer. The excitation wavelengths of the intrinsic Trp fluorescence, ANS fluorescence and ThT fluorescence were 295 nm, 380 nm and 440 nm. Parameter *A*, a sensitive parameter to reflect the position and shape of the Trp fluorescence spectra [26], was calculated by dividing the fluorescence intensity at 320 nm by that at 365 nm (I_{320}/I_{365}). The resonance Rayleigh light scattering was measured with an excitation wavelength at 295 nm [27]. The turbidity of the protein solutions was monitored by the absorbance at 400 nm (A_{400}) using an Ultraspec 4300 pro UV/Visible spectrophotometer.

2.4. Size-exclusion chromatography

Size-exclusion chromatography (SEC) analysis was conducted using a Superdex 200HR 10/30 column equipped on an ÄKTA FPLC as described previously [22,23]. In brief, the column was pre-equilibrated with buffer A at a given pH, and then 100 μl protein solutions were injected into the column and run at a flow rate of 0.4 ml/min at 4 °C. The protein concentration used for SEC analysis was 1 mg/ml. The column was calibrated using standard molecular weight markers as described elsewhere [22].

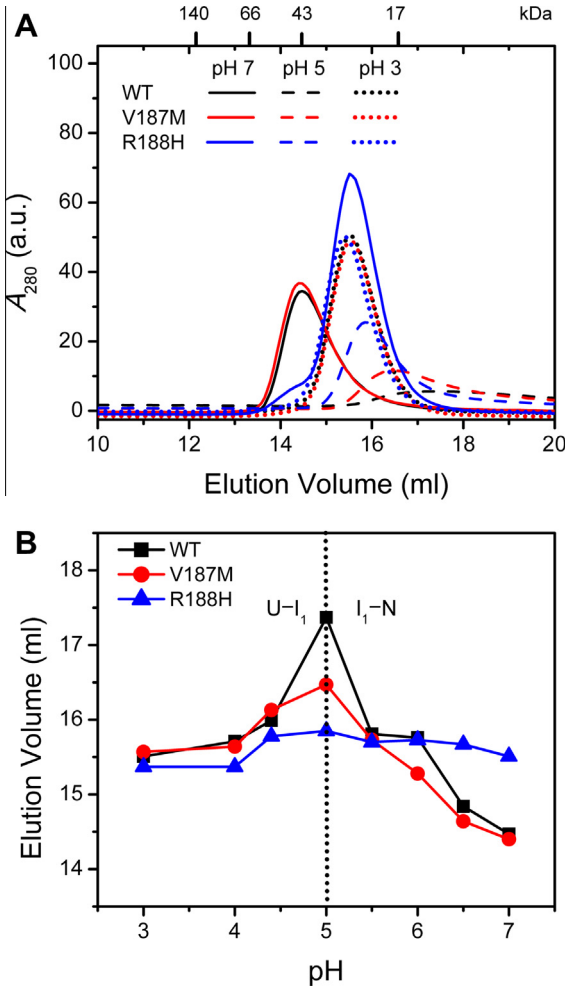

Fig. 1. Changes in the oligomeric states of the WT and mutated βB2-crystallins during acid denaturation. (A) Representative SEC profiles of the proteins. The SEC analysis was performed using a protein concentration of 1 mg/ml and carried out at 4 °C in buffer A. The positions of the standard proteins used for calibration are labeled on the top of the panel. (B) pH-dependence of the elution volumes of the main peaks in the SEC profiles. Both the WT protein and V187M eluted as a single peak under various pH conditions. The elution profiles of R188H contained a main peak from monomers and a minor peak from dimers under neutral conditions, and only the elution volume of the main peak was measured and presented.

2.5. Acid denaturation

The stock protein solutions were prepared in buffer A, pH 7.2. Acid denaturation was conducted by mixing the prepared buffer A at various pH adjusted by HCl or NaOH. The pH of the final solutions was checked after mixing. Spectroscopic experiments and SEC analysis were carried out after 1 h, 12 h or 24 h equilibration at 25 °C. The spectrum of the buffer at each pH was also recorded, and the resultant spectrum was obtained by subtracting the spectrum of the buffer from that of the protein solutions. Fitting of the data were performed by non-linear least squares algorithm using GraphPad Prism 5.01 as described previously [28].

2.6. Protein aggregation and fibrillization

The optimal conditions of the formation of amorphous aggregates and amyloid-like fibrils were screened for pH ranging from 2.0 to 5.0, temperature ranging from 25 °C to 37 °C and protein concentration ranging from 2 mg/ml to 18 mg/ml. After equilibrated for 24 h, turbidity and ThT fluorescence were determined using diluted samples with a protein concentration of 0.2 mg/ml. For the screening of the optimal pH and temperature conditions, a solution volume of 10 μl was used. The samples were sealed in tubes and were incubated simultaneously in a water bath. For the protein concentration-dependent fibrillization analysis, the proteins were incubated at pH 3.0 with a solution volume of 50 μl to minimize the experimental errors. The samples for transmission electron microscope (EM) experiments were prepared by incubating the protein solutions at 37 °C, pH 3.0, with a protein concentration of 5 mg/ml or 10 mg/ml. After 24 h incubation, the samples were diluted to 0.2 mg/ml to prepare the negatively stained EM samples, and the EM pictures were collected as described previously [23].

3. Results

Previously we have shown that in diluted solutions, the WT βB2-crystallin and V187M exist as dimers, while R188H is dominated by monomers [22]. SEC analysis was used to investigate the pH dependence of the oligomeric states of the WT and mutated βB2-crystallins. As shown in Fig. 1, only a minor shift was observed for the elution volume of R188H when the solution pH was decreased from 7 to 2, which is consistent with the monomeric nature of R188H. The elution volumes of the WT βB2-crystallin and V187M had two apparent transitions corresponding to the dissociation of the dimers and the unfolding of the monomers. The eluted peaks at pH 5 had to an apparent molecular weight of ~17 kDa, which was even smaller than that of the monomeric states of the WT βB2-crystallin and V187M. Meanwhile, the SEC peaks became flat and broad at pH 5 for all three proteins. These unusual phenomena might be caused by the unexpected interactions of the proteins with the matrix of the chromatography column. A similar delay in the elution volume has also been reported for truncated βB1-crystallins [29]. It seems that the mutations, particularly of

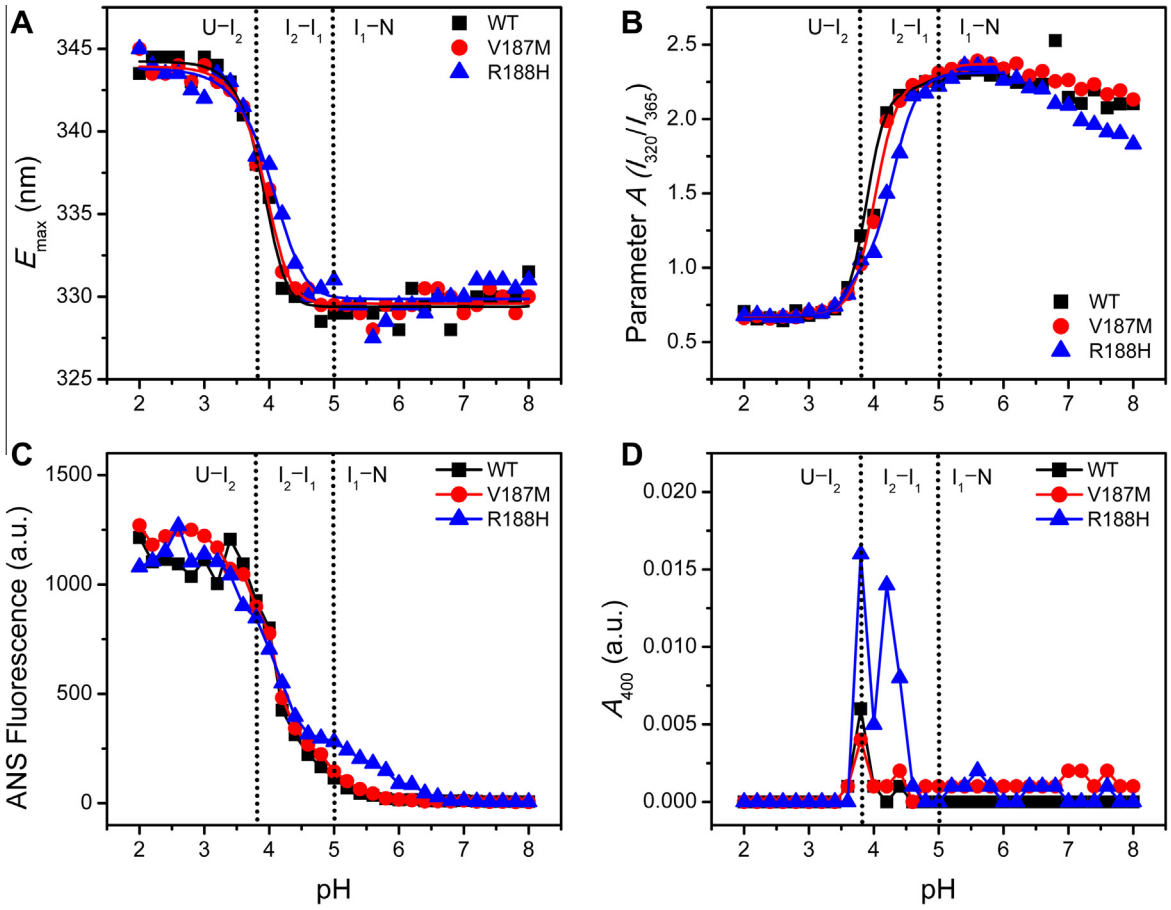

Fig. 2. Transition curves of the WT and mutated βB2-crystallins during acid-induced denaturation. (A) Maximum emission wavelength of Trp fluorescence (E_{max}). (B) Parameter A (I_{320}/I_{365}). (C) ANS fluorescence at 470 nm. (D) Turbidity monitored by the absorbance at 400 nm (A_{400}). The protein solutions with a concentration of 0.2 mg/ml were incubated at 25 °C for 12 h. The curves for samples incubated for 1 h are shown in Supplemental Fig. 1. The data between pH 2 and pH 6 in panels A and B were fitted by a three state model. The dotted lines indicate the approximate positions where the intermediate states were accumulated.

R188H, reduced the strong interactions of βB2-crystallin with the column matrix, reflecting that the mutations might modify the biophysical properties of the intermediate state appeared at pH 5.

The structural changes induced by acid denaturation were monitored by the intrinsic and extrinsic fluorescence of the proteins incubated under various pH conditions for 1 h (Supplemental Fig. 1) or 12 h (Fig. 2) at 25 °C. A comparison between the two sets of transition curves indicated that a longer incubation time was needed to fully denature the proteins in solutions with a pH between 3.6 and 4.6. A small portion of proteins tended to form aggregates when incubated at around pH 4 for 12 h (Fig. 2D and Supplemental Fig. 2), while no aggregates were observed for samples incubated for 1 h. Nonetheless, the acid-denaturation of the three proteins could be best fitted by a three-state model under pH 5, while an additional transition between pH 5 and 7 could be observed from the changes of the ANS fluorescence (Fig. 2C) as well as SEC analysis (Fig. 1). Thus the acid-induced unfolding of βB2-crystallin could be described by the following four-state model involving two unfolding intermediates (Scheme 1):

Intermediate I_1 was a monomeric state that maintained most of the native structures of βB2-crystallin and possessed a few ANS-accessible hydrophobic sites, while intermediate I_2 was partially unfolded and was prone to aggregate. The unfolded state U was dominated by disordered structures with all Trp fluorophores accessible by the solvent and contained some residual β-sheet structures (Supplemental Fig. 3).

The transition curves of V187M were almost superimposed to those of the WT protein. As for the R188H mutation, the most significant effect was the introduction of extra ANS-binding sites during the N–I_1 transition reflected by the slight increase of the ANS fluorescence (Fig. 2C and Supplemental Fig. 1C). It is worth noting that the hydrophobic imidazole group at His side-chain becomes positively charged at pH below 6. Considering that the R188H mutation dissociates βB2-crystallin into monomers in diluted solutions [22], the extra ANS-accessible sites were more likely to be introduced by the exposure of the hydrophobic sites at the subunit interface (Supplemental Fig. 4). Another impairing effect caused by R188H mutation is the destabilization of I_1 revealed by the shift of the I_1–I_2 transition curve to higher pH vales when compared to the WT protein.

$$N_2 \Leftrightarrow 2I_1 \Leftrightarrow 2I_2 \Leftrightarrow 2U\ .$$

Scheme 1.

To further evaluate the effect of mutations on the aggregatory potency of βB2-crystallin during acid denaturation, the turbidity data were recorded for samples incubated at 37 °C for 24 h (Fig. 3A). Compared to the results in Fig. 2D, the most striking difference is the serious aggregation of R188H when incubated at 37 °C under a rather wide pH range (from pH 3.2 to pH 6.4). At pH 3, all three proteins did not aggregate in diluted solutions with a protein concentration of 0.2 mg/ml. At high protein concentrations, all three proteins could form amyloid-like fibrils when incubated at 37 °C, pH 3, for 24 h (Fig. 3B). It seems that V187M had similar fibrillization properties to the WT protein. The R188H mutation slightly decreased the critical concentration of βB2-crystallin fibrillization and promoted the growth of the fibrils. Similar observation could also be seen from the EM measurements. At a protein concentration of 5 mg/ml, the WT protein only formed spherical assemblies or stick-like structures, while fibrillar or annular structures could be found for R188H. When the protein concentration was increased to 10 mg/ml, both the WT protein and R188H were extensively fibrilized, and the fibrils formed by R188H were more dense and lengthy.

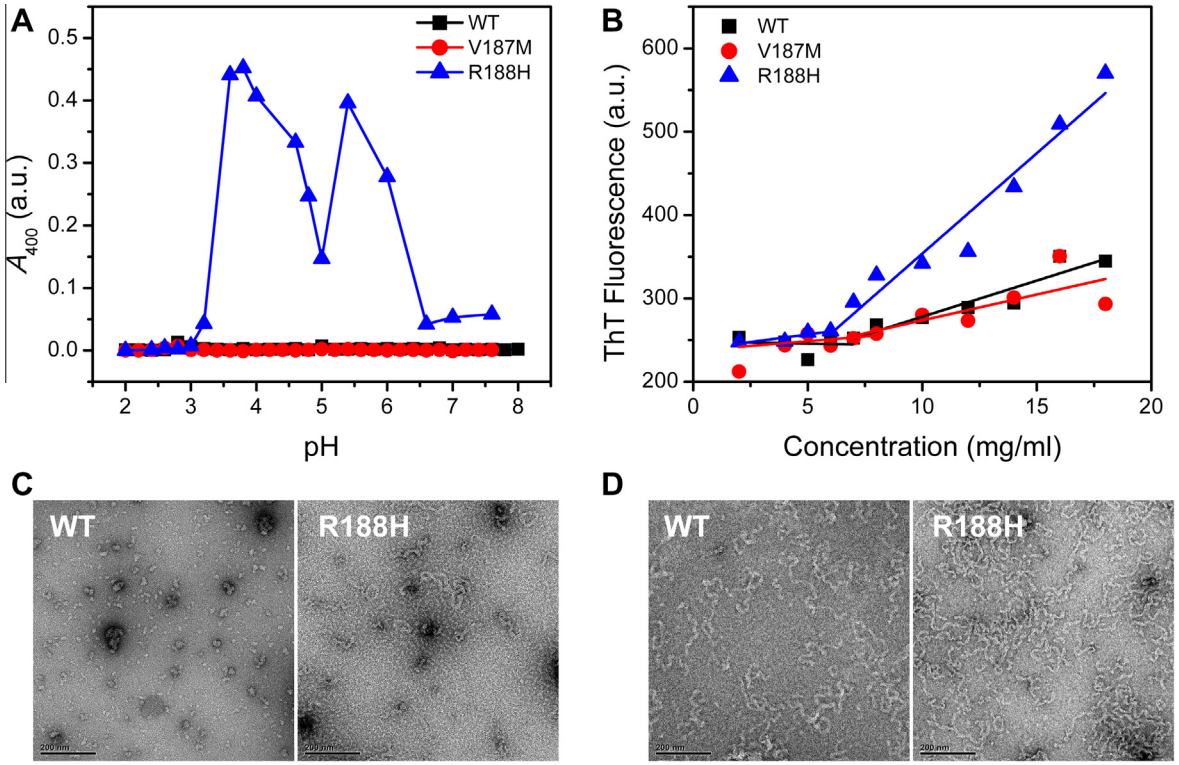

Fig. 3. Aggregation and fibrillization of the WT and mutated βB2-crystallin. (A) pH-dependence of protein aggregation monitored by turbidity. The solutions with a protein concentration of 0.2 mg/ml were incubated at 37 °C for 24 h. (B) Concentration-dependence of protein fibrillization monitored by ThT fluorescence. The proteins were incubated at 37 °C and pH 3 for 24 h. The joint-position of the two straight lines indicates the critical concentration of fibrillization, which is about 6 mg/ml for R188H and 7 mg/ml for the WT protein and V187M, respectively. (C) Negatively stained transmission EM pictures of 5 mg/ml WT protein and R188H incubated at 37 °C and pH 3 for 24 h. (D) Negatively stained transmission EM pictures of 10 mg/ml proteins incubated at 37 °C and pH 3 for 24 h.

4. Discussion

One of the key points to design novel aggregation breakers or inhibitors is to understand the molecular mechanism of aggregation. Cataract is a disease directly caused by the aggregation of crystallins in the lens. Congenital cataract-linked β/γ-crystallin mutations may lead to protein aggregation via the following mechanisms [12,30,31]: (*i*) directly decreases protein solubility by the substitution of a charged or polar residue at the surface by a hydrophobic one; (*ii*) destabilizes the protein and leads to aggregation when subjected to stresses; (*iii*) facilitates aggregation by crosslink the molecules via intermolecular disulfide bonds; (*iv*) increases the sensitivity to proteolysis and produces aggregation-prone fragments. Although many cataract-linked mutations have been found to promote β/γ-crystallin aggregation, it remains unclear whether those non-cystine substitutions do play a role in the progression of aggregation/fibrillization.

Recently it has been proposed that residues 80–163 of γD-crystallin form the core of amyloid-like fibrils under acid conditions and amorphous aggregates induced by heating [14–19]. Although the segments involved in β-crystallin aggregation remains unknown, the highly conserved structure in the β/γ-crystallin family suggested that β-crystallins might assemble into amyloid-like fibrils via a similar mechanism to γD-crystallin. It is worth noting that according to the crystal structure of γD-crystallin, residues 80–163 mainly spans the linker and most of the C-terminal domain but not the last β-strand of Greek-key motif 4 (Supplemental Fig. 5). However, both V187 and R188 locate at the last β-strand of Greek-key motif 4 in βB2-crystalllin, suggesting that these two residues might not be directly involved in the core structure formation of βB2-crystalllin aggregates/fibrils. This deduction is supported by the observations that V187M exhibited similar behavior to the WT protein and R188H only affected the aggregatory potency but not the morphology of mature βB2-crystalllin fibrils. Furthermore, the different behaviors between R188H and V187M/WT indicated that His188 could play a regulatory role in R188H aggregation/fibrillization.

The structural basis of the regulatory role of His188 in R188H aggregation is difficult to elucidate since only the repeated β-sheet packing of the fibrils/aggregates has a possibility to be studied by structural methods such as solid-state NMR. Nonetheless, some clues could be obtained from the current and previous results. Previous molecular dynamic modeling studies have shown that the V187M and R188H mutations do not affect the fold of the Greek-key motifs of βB2-crystalllin [22]. Spectroscopic studies in this research also indicated that the three proteins possessed similar secondary and tertiary structures at pH 3 (Supplemental Fig. 3). Thus it seems that the R188H mutation did not influence the residual structure of the monomeric species prior to aggregate. Moreover, under acidic conditions, the hydrophobic imidazole group in histidine is hydrophilic due to the protonation of the amine group at pH below 6. Thus the promotion effect of the R188H mutation was not due to an alternation in the charges of the molecules. Considering that the R188H mutation facilitates βB2-crystalllin tetramerization at high protein concentrations [22] and that β-strands in native structures may also be involved in the formation of intermolecular β-sheets [16–19], it is possible that His188 contributed to the progression of R188H aggregation/fibrillization by stabilizing the intermolecular interactions around the core β-sheet structures.

In conclusion, in this research we used acid denaturation as a model system to separate the effects of cataract-linked mutations on protein structure, stability, aggregation and fibrillization. The distinct effect of the two adjacent point mutations on βB2-crystalllin aggregation and fibrillization indicated that cataract-linked mutations might promote protein aggregation via quite different mechanisms. That is, the V187M mutation destabilized βB2-crystalllin but did not influence the aggregation mechanism, while the R188H mutation not only decreased βB2-crystalllin stability but also regulated the progression of aggregation/fibrillization. The dual effects of the R188H mutation made the mutated protein intrinsically aggregation-prone. Our results suggested that the disease-linked mutations might accelerate protein aggregation/fibrillization by stabilizing the intermolecular interactions among regions flanking the core structure of the aggregates/fibrils.

Acknowledgments

This study was supported by funds from the Ministry of Science and Technology of China (2010CB912402 and 2012BAI08B01), National Natural Science Foundation of China (81371001), Zhejiang Key Innovation Team Project of China (2009R50039) and Zhejiang Key Laboratory Fund of China (2011E10006). The authors thank Sha Wang for helpful suggestions.

Appendix A. Supplementary data

Supplementary data associated with this article can be found, in the online version, at http://dx.doi.org/10.1016/j.bbrc.2014.03.119.

References

[1] C.M. Dobson, Protein folding and misfolding, Nature 426 (2003) 884–890.
[2] M.A. DePristo, D.M. Weinreich, D.L. Hartl, Missense meanderings in sequence space: a biophysical view of protein evolution, Nat. Rev. Genet. 6 (2005) 678–687.
[3] E.M. Sontag, W.I. Vonk, J. Frydman, Sorting out the trash: the spatial nature of eukaryotic protein quality control, Curr. Opin. Cell Biol. 26C (2014) 139–146.
[4] G.B. Benedek, Cataract as a protein condensation disease: the proctor lecture, Invest. Ophthalmol. Vis. Sci. 38 (1997) 1911–1921.
[5] H. Bloemendal, The vertebrate eye lens, Science 197 (1977) 127–138.
[6] S. Bassnett, Lens organelle degradation, Exp. Eye Res. 74 (2002) 1–6.
[7] U.P. Andley, Crystallins in the eye: function and pathology, Prog. Retin. Eye Res. 26 (2007) 78–98.
[8] R. Jaenicke, Stability and folding of ultrastable proteins: eye lens crystallins and enzymes from thermophiles, FASEB J. 10 (1996) 84–92.
[9] J. Horwitz, a-Crystallin can function as a molecular chaperone, Proc. Natl. Acad. Sci. U.S.A. 89 (1992) 10449–10453.
[10] J.F. Hejtmancik, Congenital cataracts and their molecular genetics, Semin. Cell Dev. Biol. 19 (2008) 134–149.
[11] J. Graw, Genetics of crystallins: cataract and beyond, Exp. Eye Res. 88 (2009) 173–189.
[12] K.L. Moreau, J.A. King, Protein misfolding and aggregation in cataract disease and prospects for prevention, Trends Mol. Med. 18 (2012) 273–282.
[13] H. Ecroyd, J.A. Carver, Crystallin proteins and amyloid fibrils, Cell. Mol. Life Sci. 66 (2009) 62–81.
[14] M.S. Kosinski-Collins, J. King, In vitro unfolding, refolding, and polymerization of human γD crystallin, a protein involved in cataract formation, Protein Sci. 12 (2003) 480–490.
[15] K. Papanikolopoulou, I. Mills-Henry, S.L. Tho, Y.T. Wang, A.A.R. Gross, D.A. Kirschner, S.M. Decatur, J. King, Formation of amyloid fibrils in vitro by human γD-crystallin and its isolated domains, Mol. Vis. 14 (2008) 81–89.
[16] P. Das, J.A. King, R. Zhou, Aggregation of gamma-crystallins associated with human cataracts via domain swapping at the C-terminal beta-strands, Proc. Natl. Acad. Sci. U.S.A. 108 (2011) 10514–10519.
[17] S.D. Moran, S.M. Decatur, M.T. Zanni, Structural and sequence analysis of the human γD-crystallin amyloid fibril core using 2D IR spectroscopy, segmental ^{13}C labeling, and mass spectrometry, J. Am. Chem. Soc. 134 (2012) 18410–18416.
[18] S.D. Moran, A.M. Woys, L.E. Buchanan, E. Bixby, S.M. Decatur, M.T. Zanni, Two-dimensional IR spectroscopy and segmental ^{13}C labeling reveals the domain structure of human γD-crystallin amyloid fibrils, Proc. Natl. Acad. Sci. U.S.A. 109 (2012) 3329–3334.
[19] S.D. Moran, T.O. Zhang, M.T. Zanni, An alternative structural isoform in amyloid-like aggregates formed from thermally denatured human γD-crystallin, Protein Sci. 23 (2014) 321–331.
[20] M.E. Mothobi, S. Guo, Y. Liu, Q. Chen, A.S. Yussuf, X. Zhu, Z. Fang, Mutation analysis of congenital cataract in a Basotho family identified a new missense allele in *CRYBB2*, Mol. Vis. 15 (2009) 1470–1475.
[21] N. Weisschuh, S. Aisenbrey, B. Wissinger, A. Riess, Identification of a novel *CRYBB2* missense mutation causing congenital autosomal dominant cataract, Mol. Vis. 18 (2012) 174–180.

[22] K. Zhang, W.-J. Zhao, X.-Y. Leng, S. Wang, K. Yao, Y.-B. Yan, The importance of the last strand at the C-terminus in βB2-crystallin stability and assembly, Biochim. Biophys. Acta Mol. Basis Dis. 2014 (1842) 44–55.
[23] J. Xu, S. Wang, W.-J. Zhao, Y.-B. Xi, Y.-B. Yan, K. Yao, The congenital cataract-linked A2V mutation impairs tetramer formation and promotes aggregation of βB2-crystallin, PLoS ONE 7 (2012) e51200.
[24] M.M. Bradford, A rapid and sensitive method for the quantitation of microgram quantities of protein utilizing the principle of protein–dye binding, Anal. Biochem. 72 (1976) 248–254.
[25] W. Zhang, H.-C. Cai, F.-F. Li, Y.-B. Xi, X. Ma, Y.-B. Yan, The congenital cataract-linked G61C mutation destabilizes γD-crystallin and promotes non-native aggregation, PLoS ONE 6 (2011) e20564.
[26] K.K. Turoverov, S.Y. Haitlina, G.P. Pinaev, Ultra-violet fluorescence of actin. Determination of native actin content in actin preparations, FEBS Lett. 62 (1976) 4–6.
[27] G.-J. He, A. Zhang, W.-F. Liu, Y. Cheng, Y.-B. Yan, Conformational stability and multistate unfolding of poly(A)-specific ribonuclease, FEBS J. 276 (2009) 2849–2860.
[28] S. Wang, X.-Y. Leng, Y.-B. Yan, The benefits of being β-crystallin heteromers: βB1-crystallin protects βA3-crystallin against aggregation during co-refolding, Biochemistry 50 (2011) 10451–10461.
[29] O.A. Bateman, N.H. Lubsen, C. Slingsby, Association behaviour of human βB1-crystallin and its truncated forms, Exp. Eye Res. 73 (2001) 321–331.
[30] V.P.R. Vendra, G. Agarwal, S. Chandani, V. Talla, N. Srinivasan, D. Balasubramanian, Structural integrity of the Greek key motif in βγ-crystallins is vital for central eye lens transparency, PLoS ONE 8 (2013) e70336.
[31] S. Wang, W.-J. Zhao, H. Liu, H. Gong, Y.-B. Yan, Increasing βB1-crystallin sensitivity to proteolysis caused by the congenital cataract-microcornea syndrome mutation S129R, Biochim. Biophys. Acta Mol. Basis Dis. 2013 (1832) 302–311.